Metabolic Engineering 73 (2022) 124–133

Contents lists available at ScienceDirect

Metabolic Engineering

journal homepage: www.elsevier.com/locate/meteng

Single cell mutant selection for metabolic engineering of actinomycetes

Amir Akhgari [a,#,†], Bikash Baral [a,#], Arina Koroleva [a], Vilja Siitonen [a], David P. Fewer [b], Charles E. Melançon III [c,1], Jani Rahkila [d], Mikko Metsä-Ketelä [a,*]

[a] Department of Life Sciences, University of Turku, Turku, FIN, 20014, Finland
[b] Department of Microbiology, University of Helsinki, Helsinki, FIN, 00014, Finland
[c] Department of Chemistry and Chemical Biology, University of New Mexico, Albuquerque, NM, 87131-0001, USA
[d] Instrument Centre, Faculty of Science and Engineering, Åbo Akademi University, Turku, FIN, 20500, Finland

ARTICLE INFO

Keywords:
Amycolatopsis
Streptomyces
Fluorescence-activated cell sorting
Polyketide
Protein production

ABSTRACT

Actinomycetes are important producers of pharmaceuticals and industrial enzymes. However, wild type strains require laborious development prior to industrial usage. Here we present a generally applicable reporter-guided metabolic engineering tool based on random mutagenesis, selective pressure, and single-cell sorting. We developed fluorescence-activated cell sorting (FACS) methodology capable of reproducibly identifying high-performing individual cells from a mutant population directly from liquid cultures. Actinomycetes are an important source of catabolic enzymes, where product yields determine industrial viability. We demonstrate 5-fold yield improvement with an industrial cholesterol oxidase ChoD producer *Streptomyces lavendulae* to 20.4 U g^{-1} in three rounds. Strain development is traditionally followed by production medium optimization, which is a time-consuming multi-parameter problem that may require hard to source ingredients. Ultra-high throughput screening allowed us to circumvent medium optimization and we identified high ChoD yield production strains directly from mutant libraries grown under preset culture conditions. Genome-mining based drug discovery is a promising source of bioactive compounds, which is complicated by the observation that target metabolic pathways may be silent under laboratory conditions. We demonstrate our technology for drug discovery by activating a silent mutaxanthene metabolic pathway in *Amycolatopsis*. We apply the method for industrial strain development and increase mutaxanthene yields 9-fold to 99 mg l^{-1} in a second round of mutant selection. In summary, the ability to screen tens of millions of mutants in a single cell format offers broad applicability for metabolic engineering of actinomycetes for activation of silent metabolic pathways and to increase yields of proteins and natural products.

1. Introduction

Actinomycetes are filamentous Gram-positive bacteria that are widely utilized in diverse industrial biotechnology applications. Approximately two thirds of antibiotics and one third of anti-cancer agents in clinical use are natural products produced by actinomycetes or their semi-synthetic derivatives (Newman and Cragg, 2020). Microbial natural products are widely used as immunosuppressants (Mann, 2001), antiparasitic (Shiomi and Omura, 2004), and antifungal agents (Thirsk and Whiting, 2002). However, improved biologically active compounds are urgently needed to combat the emergence of antibiotic resistance in microbial pathogens (Årdal et al., 2019) and to alleviate the side-effects commonly associated with cancer chemotherapy agents (van der Zanden et al., 2021). Actinomycetes are likely to remain a critical source of new drug candidates (Genilloud, 2017), since genome sequencing projects have identified a tremendous number of unstudied biosynthetic gene clusters (BGCs) that could encode novel secondary metabolites (Baral et al., 2018). Methods for the bioinformatic identification of BGCs have become increasingly sophisticated (Albarano et al., 2020), but isolation of the associated natural products has remained highly challenging. Genome mining driven drug discovery is complicated, because the majority of BGCs are silent under laboratory

* Corresponding author.
E-mail address: mianme@utu.fi (M. Metsä-Ketelä).
† VTT Technical Research Centre of Finland Ltd., Tietotie 2, FIN-02044, Espoo, Finland.
1 Applied Biomedical Science Institute, San Diego, CA 92127.
# Equal contribution.

https://doi.org/10.1016/j.ymben.2022.07.002
Received 28 January 2022; Received in revised form 31 May 2022; Accepted 1 July 2022
Available online 7 July 2022

monoculture conditions. Many pathways require specific environmental signals for activation and are governed by complex regulatory cascades (Van Wezel and McDowall, 2011). Several techniques for activation of BGCs have been developed, but to date no single widely applicable methodology for targeted activation of metabolic pathways has emerged (Medema et al., 2021).

Actinomycetes play an important role in soil ecology, where they have adapted to decompose complex organic plant, anthropod and crustacean polymers (van der Meij et al., 2017). The proteins involved in these processes provide a significant fraction of commercially available enzymes used particularly in paper and pulp (e.g. xylanases and cellulases) and detergent (e.g. lipases and amylases) manufacturing (Prakash et al., 2013). Numerous enzyme applications can also be found in the food and beverage (e.g. proteases and glucose oxidase) and textile (e.g. pectinases and peroxidases) industries (Mukhtar et al., 2017). Many medical diagnostic laboratories also depend on enzyme use in bioassays (e.g. cholesterol oxidase) (Yamada et al., 2019). Cholesterol oxidase ChoD is also utilized in the bioconversion of non-steroidal compounds, allylic alcohols and sterols, and in the chemoenzymatic synthesis of hormones and steroidal drug intermediates (Yamada et al., 2019).

The manufacturing of both microbial natural products and proteins occurs in an enclosed bioreactor. Therefore product yields are key determinants for the commercial viability of the manufacturing process (Bandyopadhyay et al., 2017). Microbial strain development is an unceasing endeavor in pharmaceutical companies, where the yields of secondary metabolites have been increased from few tens of milligrams per liter in wild type strains to grams per liter in industrial production strains (Adrio and Demain, 2006). Traditionally this decade-long process involves generation of millions of mutants by random mutagenesis followed by individual cultivation of each mutant strain to assess production profiles and yields (Miethke et al., 2021). Cultivating thousands of actinomycetes strains in flask cultures is laborious and challenging to scale up even with high-throughput screening technologies. Once best producing mutants have been identified, the composition of medium ingredients needs to be optimized for high-yield production (Miethke et al., 2021). This represents another time-consuming challenge, since medium optimization is a multi-parameter problem, where modification of one component influences the ideal concentrations of the other medium ingredients (Bandyopadhyay et al., 2017).

One attractive means of accelerating strain development has been to use reporter genes to focus on mutants with increased transcription of target genes (Askenazi et al., 2003; Guo et al., 2015; Li et al., 2018; Wang et al., 2016; Xiang et al., 2009). Increased yields of lovastatin (Askenazi et al., 2003) and natamycin (Wang et al., 2016) have been reported by linking transcription from the BGCs to the survival of the microbes under selection. A double reporter system was developed to reduce the number of false positive mutants to screen improved clavulanic acid producing mutants (Xiang et al., 2009). Reporter guided mutant selection has also been utilized for the activation of silent BGCs with jadomycin (Guo et al., 2015), gaudimycin (Guo et al., 2015), streptothricin (Li et al., 2018), geosmin (Li et al., 2018) and strevertene (Li et al., 2018) providing examples. Biosensors based on BGC situated repressor proteins have been used in the activation of coelimycin (Sekurova et al., 2021) pathway.

These studies have shown the value of reporter genes in strain development of actinomycetes. However, all depend on the detection of improved mutants on cultivation plates (Askenazi et al., 2003; Bandyopadhyay et al., 2017; Minas, 2005; Wang et al., 2016). This not only influences the throughput of the methodology, but also disassociates the screening conditions from the production environment in the bioreactor. Fluorescence-activated cell sorting (FACS) is an ideal method for sorting liquid cultures of heterogeneous mixtures of biological cells (Binder et al., 2012) and is routinely used in strain development of yeast (Wagner et al., 2018) and selected bacteria (Wendisch, 2014). However, actinomycetes are filamentous bacteria that grow as branching mycelia, which hinders the use of FACS (Bai et al., 2015; Cao et al., 2018). A key problem is that the 70 μM nozzle size of the FACS instruments is typically orders of magnitude smaller than typical *Streptomyces* mycelia (e.g. 260–950 μM) (Manteca et al., 2008; van Veluw et al., 2012). This limitation was circumvented by the use of protoplasts to pass through the instrument (Bai et al., 2015). However, the technique has ultimately not gained wide use, possibly because of the fragility of protoplasts and very low survival rates following cell sorting. Here we have developed facile methodology that does not use protoplasts to allow reporter guided screening of actinomycetes by FACS. We demonstrate that single cell mutant selection (SCMS), which couples traditional mutagenesis to selection pressure and ultra-high throughput screening, can be used to activate silent BGCs, to increase the yields of proteins and secondary metabolites, and replace medium optimization.

2. Results

General workflow. A reporter construct is assembled in the first step by cloning the target promoter sequence in front of a double reporter plasmid pS-GK, constructed in the wide host range integrative pSET152 vector (Bierman et al., 1992) (Fig. 1a and Supplementary Text). Two alternative versions with antibiotic resistance markers *kan* (Nakano et al., 1984) or *hyg* (Zalacain et al., 1986) to impose selection using either kanamycin and hygromycin, respectively, are available. Importantly, the selection markers encode acyl transferase and kinase enzymes that inactivate their target antibiotics (Ramirez and Tolmasky, 2010), which provides a link between the transcription level of the resistance gene and survival of the bacterial strain under elevated concentrations of the antibiotic. Resistance markers that modify the target site of the antibiotics would not provide such concentration dependent response. For the second reporter gene, we chose superfolder Green Fluorescent Protein (sfGFP) to allow screening by FACS. The reporter genes are insulated using two strong terminator sequences, a synthetic T4 kurz (Horbal et al., 2018) and a natural terminator ECK120029600 (Chen et al., 2013).

In the second step, classical mutagenesis is carried out to introduce genome-wide mutations and to generate a mutant library (Fig. 1b). Positive mutants with increased transcription from the target promoter are enriched using selection (Fig. 1c) and subjected to ultra-high throughput screening by FACS to find best performing mutants (Fig. 1d). As a positive control for FACS, we devised plasmid pS-GK (Fig. 2a and Supplementary Fig. 1), where the reporter genes are cloned under the strong synthetic promoter SP44 (Bai et al., 2015). Pure cultures of mutants are initially ranked based on fluorescence (Fig. 1e), followed by quantification of target protein (Fig. 1f) or metabolite level (Fig. 1g). The full protocol is described in detail in Supplementary Text.

Strain development for protein overproduction. First we focused on production of a cholesterol oxidase enzyme ChoD by an industrial strain *S. lavendulae* YAKB-15 (Yamada et al., 2019), which has been mutagenized for high yield production. The promoter sequence of the operon including *choD* (Fig. 2b) was cloned into the reporter construct in *Escherichia coli* and the resulting plasmid pS_GK_ChoD (Fig. 2c and Supplementary Fig. 2) was introduced to *S. lavendulae* YAKB-15. The exconjugants could withstand kanamycin concentrations to a maximum of 50 μg ml^{-1} in the production medium, reflecting the natural transcriptional level of *choD*. Next we generated a mutant library of *S. lavendulae* YAKB-15/pS_GK_ChoD by treatment of spores with ethyl methanesulfonate. The mutant library was used to inoculate parallel cultivations in Y production medium (Yamada et al., 2019) supplemented with varying concentrations (50–400 μg ml^{-1}) of kanamycin, with the objective of enriching best performing mutants that tolerate high concentrations of the antibiotic and reducing the library size by killing off undesired low or non-producing mutants. Bacterial growth could still be observed in cultures with 400 μg ml^{-1} kanamycin, which demonstrated an 8.0-fold increase in the tolerance of the mutant library towards kanamycin.

In order to utilize FACS, we hypothesized that fragmentation of

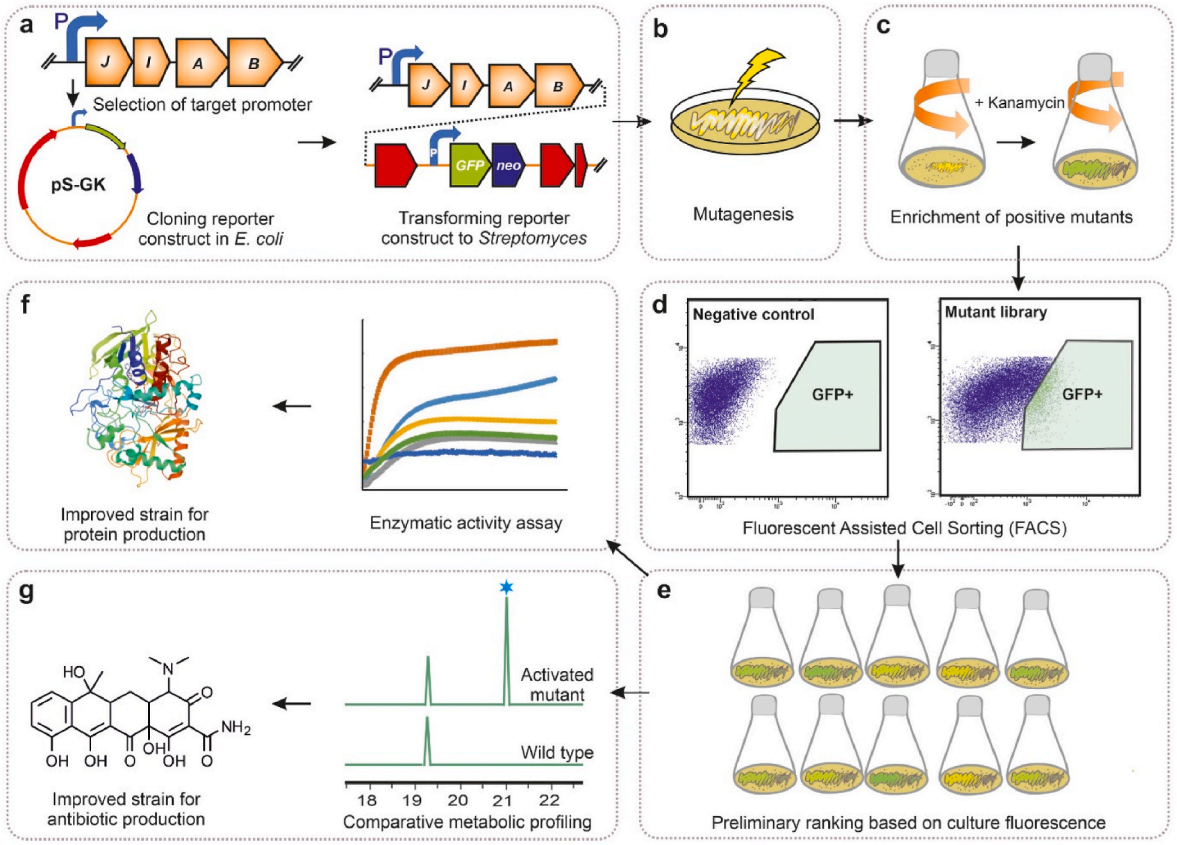

Fig. 1. Single cell mutant selection platform for metabolic engineering. The strain improvement pipeline includes **a**, Construction of reporter plasmid by selecting a promoter region (P) from target gene(s), cloning the promoter in *E. coli* and conjugation of the plasmid into the production strain. **b**, Introduction of genome-wide mutations by mutagenesis to generate overproducing strains. **c**, Transfer of the mutant library to a liquid culture and addition of antibiotics to impose selection to enrich positive mutants. **d**, Screening millions of mutants by FACS to find strains with highest fluorescence signal. Mutant libraries display a wide range of fluorescence values (x-axis) in comparison to a non-mutated negative control strain. Each dot represents a single cell. **e**, Preliminary analysis of pure cultures by fluorometer to rank mutants. **f**, Enzymatic activity assays to find best performing strain for protein overproduction or **g**, Comparative metabolic profiling to find improved strains for production of microbial natural products.

mycelium by sonication (Baltz, 1978; Stonesifer and Baltz, 1985) might be sufficient to allow single cells to pass through the nozzles of the instruments. The combination of sample filtration (Supplementary Fig. 3) and careful instrument gating using two-step doublet discrimination (Supplementary Fig. 4) allowed us to analyze actinomycete single cells by FACS. We conducted propidium iodide (PI) staining experiments with altered sonication pulses (5–30 s) to assess the ratio of dead and live cells during cell sorting (Supplementary Figs. 5a–h). Actinomycetes could withstand the sonication process well with a significant 40% fraction of live cells inside the instrument after short 5–10 s sonication pulses. Recovery of sorted cells was analyzed by harvesting 100 individual cells and counting colony forming units (Supplementary Figs. 5i–j), which revealed good over 80% recovery for short 5 s pulses. However, noticeable strain-to-strain variation could be observed with longer 30 s pulses, where recovery rates of *S. lavendulae*/pSGK-ChoD diminished to approximately 20% (Supplementary Figs. 5a–h).

In order to find mutant strains overexpressing *choD*, we screened approximately 2×10^7 cells from the enriched *S. lavendulae* YAKB-15/pS_GK_ChoD mutant library to find individual mutants with the highest sfGFP fluorescence. Positive mutants expressing sfGFP were harvested and analyzed for cholesterol oxidase activity in flask cultures in Y production medium (Fig. 2d). The mutant *S. lavendulae* Y1 (1) displayed 1.8-fold increase in yield of ChoD (7.7 U g^{-1}) in comparison to *S. lavendulae* YAKB-15 (4.1 U g^{-1}).

Next we performed two more rounds of SCMS using the best performing mutant from the previous round as starting material. Single cells derived from second and third round mutagenesis and selection were resistant to 800 μg ml^{-1} and 900 μg ml^{-1} kanamycin, respectively. In total, three rounds of SCMS resulted in 5.0-fold yield enhancement in mutant *S. lavendulae* Y3 (10) (20.4 U g^{-1}) in comparison to *S. lavendulae* YAKB-15.

Strain improvement in preselected medium. The production of cholesterol oxidase ChoD is tightly regulated in *S. lavendulae* YAKB-15 and is linked to the presence of whole yeast cells in the Y culture medium (Yamada et al., 2019). Establishing optimal culture conditions is a necessity for industrial production of natural products and proteins by actinomycetes, since production levels fluctuate greatly in response to changing conditions (Bandyopadhyay et al., 2017). Since media optimization is a complex multi-parameter problem that may requires hard to source ingredients not suitable for industrial use, we concluded that the ability to take advantage of concentration-dependent antibiotic selection in strain development could be used to change the paradigm: instead of finding optimal culture conditions, SCMS could be used to find individual mutants that have a tendency for high yield production under preset culture conditions. Selection is the most efficient method to detect rarely occurring events and would allow identification of mutants that have adapted for high-yield production under conditions conforming to industrial conventions.

We selected yeast extract-based GYM medium, where the production yields of ChoD (0.4 U g^{-1}) are low in *S. lavendulae* YAKB-15. The three rounds of single cell mutant selection led to continuously improved product titers (Fig. 2e) and generation of a mutant strain *S. lavendulae* GYM3 (2), where the production of ChoD was 2.2-fold higher (9.1 U g^{-1}) in GYM medium than from *S. lavendulae* YAKB-15 under optimized

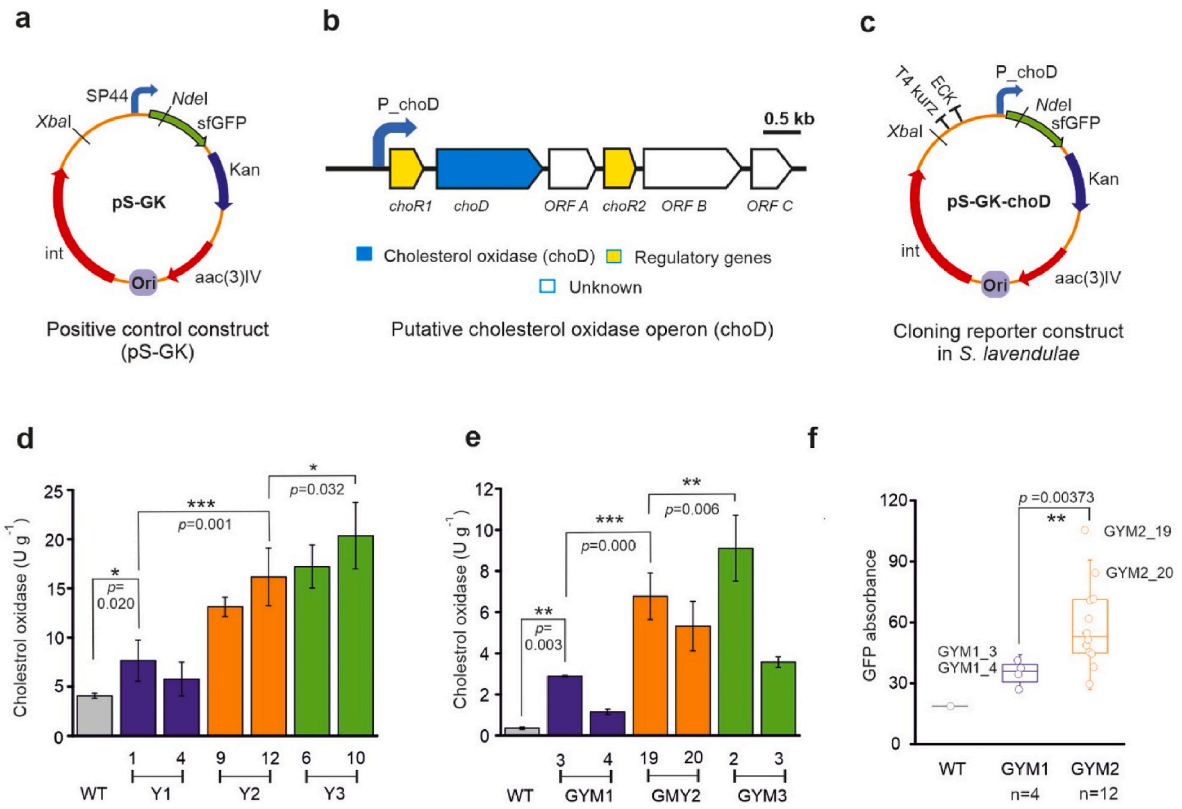

Fig. 2. Improving ChoD protein production in *S. laevendulae* YAKB-15. a, Plasmid map for the positive control construct pS-GK containing the strong synthetic promoter SP44. Kanamycin resistance gene *kan* and *sfGFP* encoding superfolder Green Fluorescent Protein were used for selection and screening, respectively. Terminators T4 kurz (Horbal et al., 2018) and ECK120029600(Chen et al., 2013) were used to insulate the promoter-probe construct. **b**, Structure of the *choD* operon and selection of the promoter region. **c**, The promoter for the *choD* operon was ordered as synthetic DNA and cloned as *Xba*I – *Nde*I fragment to generate the activation construct pS_GK_Chod. **d**, Cholesterol oxidase activity measurements from cultures grown in Y medium depicting increased yields of ChoD in three rounds of SCMS. Two mutants are shown for each round (Y1, first round; Y2, second round; Y3, third round) and the best performing mutant was selected for subsequent rounds of SCMS. **e**, Cholesterol oxidase activity measurements from cultures of two best mutants grown in GYM medium depicting increased yields of ChoD in three rounds of SCMS (GYM1, first round; GYM2, second round; GYM3, third round). **f**, Preselection of best stains after steak plating and fluorescence analysis in GYM medium. Lines depict the lineages of the strains in **d** and **e**. Significant differences were analyzed by one-way ANOVA with Tukey's post hoc analysis, and $p < 0.05$ was considered statistically significant. $^{***}p < 0.001$, $^{**}p < 0.01$, $^{*}p < 0.05$.

culture conditions in Y medium (4.1 U g^{-1}). The mutant libraries were found to be resistant to 200 μg ml^{-1}, 400 μg ml^{-1} and 600 μg ml^{-1} kanamycin in the first, second and third round of mutation, respectively, demonstrating the importance of the enrichment steps.

During strain development we noted fluctuations in ChoD production levels in strains acquired from *S. lavendulae* GYM1 and GYM2 mutant libraries, which we surmised might be due to acquisition of doublets instead of single cells by FACS. Product yields were stabilized through streak plating of cells acquired by FACS and introduction of a preliminary ranking step based on overall culture fluorescence (Fig. 2f). Higher fluorescence values (e.g. GYM1_3 and GYM2_19) correlated well with higher ChoD yields (Fig. 2e and f), which offers a rapid test to rank positive hits harvested by FACS directly from cultures.

Activation of a silent metabolic pathway. We used the software package *Dynamite* (Ogasawara et al., 2015) to identify all putative type II polyketide BGCs in the NCBI databank. The resulting ~500 unstudied BGCs were scored and prioritized for predicted chemical novelty. Among these, the target BGC in *Amycolatopsis orientalis* NRRL F3213 was assessed to be transcriptionally silent based on the absence of typical type II polyketide UV/Vis spectral signatures, which typically display absorbance in the visible 400–600 nm range, in GYM medium extracts. The BGC (Fig. 3a and Supplementary Table 1) was predicted to encode a tetracycline-type compound based on ketosynthase (KS) α and β active site motifs and the complement of cyclase genes including a bifunctional aromatase-cyclase and *oxyN*-like cyclase genes (Pickens and Tang, 2010). However, the presence of a priming ketosynthase III (KSIII) from an uncharacterized clade along with the absence of an *oxyD*-like amidotransferase indicated a new non-acetate primed tetracycline core structure, while the presence of a high number of oxidative and reductive enzymes suggesting extensive tailoring of the polyketide.

We proceeded to clone the promoter region of an operon controlling the expression of the SARP-family regulatory gene (Wietzorrek and Bibb, 1997) and the essential, translationally coupled, KS_{α} and KS_{β} responsible for synthesis of the polyketide scaffold, to generate the activation construct pSGKP45 (Fig. 3a and Supplementary Fig. 6) in *E. coli*. Introduction of the plasmid to *A. orientalis* NRRL F3213 did not induce formation of a sfGFP signal, reinforcing our hypothesis that the BGC was not transcribed under laboratory conditions. In order to activate the metabolic pathway, we proceeded to carry out mutagenesis of spores by UV radiation, enrichment under kanamycin selection (200 μg ml^{-1}) and cell sorting by FACS (Fig. 3b). Single cells with positive sfGFP signal were harvested and grown in liquid cultures and on plates (Fig. 3c), which revealed phenotypically distinct mutants producing dark pigmented metabolites. We performed transcriptional analysis of the KS_{α} gene by RT-PCR in order to validate that the targeted pathway had been activated in the mutant (Fig. 3d–f). The experiments confirmed that the BGC was active in the *A. orientalis* UV1(3) mutant, but not in the wild type (Fig. 3e). Time-course analysis indicated that the activation occurred on day four and the pathway remained active until the end of the cultivation period on day eight (Fig. 3f).

Comparative metabolic analysis of culture extract by HPLC-UV/Vis (Fig. 4a) revealed that *A. orientalis* UV1(3) produced two main

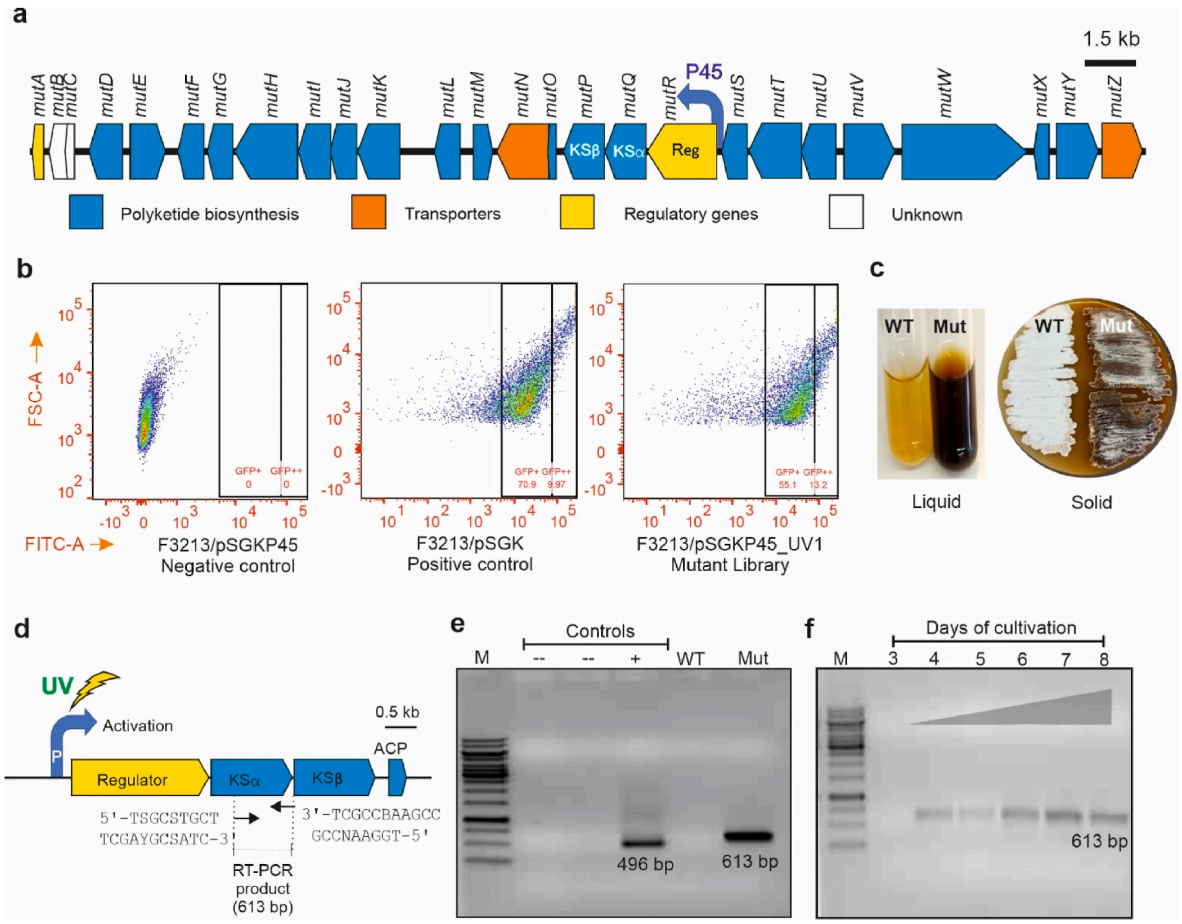

Fig. 3. Activation of a mutaxanthene BGC in *A. orientalis* NRRL F3213. a, Organization of the aromatic type II polyketide BGC detected in *A. orientalis* NRRL F3213. The promoter targeted in SCMS is highlighted. **b**, FACS analysis of an enriched mutant library of *A. orientalis* NRRL F3213/pSGKP45 demonstrated enhanced sfGFP signal in a fraction of the mutants. Non-mutated *A. orientalis* NRRL F3213/pSGKP45 was used as a negative control, while *A. orientalis* NRRL F3213/pSGK, where the fluorescence signal is generated through expression of *sfGFP* from a strong constitutive synthetic promoter SP44, was used as a positive control. Each dot represents a single cell. **c**, Example of the phenotype of a GFP-positive mutant strain *A. orientalis* UV1(3) that produces pigmented metabolites in liquid cultures and on plates in contrast to the wild type strain. **d**, Schematic representation of the binding sites of primers used for detection of transcription from the core KS_{α} gene by RT-PCR. **e**, Confirmation of the cluster activation as detected by RT-PCR. Negative controls (lane 2 and 3) were reaction mixtures without reverse transcriptase enzyme and without RNA template, respectively. As a positive control, *in vitro*-transcribed human glyceraldehyde-3-phosphate dehydrogenase (GAPDH) control RNA was utilized (lane 4) that gave the product of size 496 bp. Detection of activated BGC on day 7 in *A. orientalis* UV1(3), where the expected 613 bp band is observed (lane 6). No products were observed in analysis of the wild type strain (lane 5). **f**, Time course analysis indicates that the BGC is activated on day 4 and transcription continues until day 8 in *A. orientalis* UV1(3).

secondary metabolites **1** and **2** (Fig. 4b) not synthesized by the parental wild type strain. Furthermore, we noted that **1** was converted to **3** (Fig. 4b) during extractions in the presence of ammonium acetate. The mutant strain was cultivated in large-scale to obtain sufficient material for structure elucidation by NMR (Supplementary Tables 2–6) and HR-MS (Supplementary Fig. S7). The combined 1H and 13C, HSQCED, HMBC and 1,1-ADEQUATE NMR data confirmed that **1**, **2** and **3** were known polyketide natural products mutaxanthenes A, B and D, respectively (Derewacz et al., 2013). Conversion of **1** to its enamine congener **3** in pH ~6.6 ammonium acetate buffer has been noted previously (Derewacz et al., 2013).

Biosynthesis of mutaxanthenes. Analysis of the '*mut*' BGC provided further confirmation that the activated pathway is responsible for mutaxanthene biosynthesis. A mutaxanthene biosynthetic pathway has previously been reported in *Nocardiopsis* sp. FU40, but the nucleotide sequence was not deposited in public sequence repositories (Derewacz et al., 2013). Comparison of sequences obtained from the authors (Brian O. Bachmann, personal communication) revealed that the minimal polyketide synthases (KS_{α}, KS_{β} and acyl carrier protein) of the two BGCs shared high 96.5% nucleotide sequence identity. As predicted, the biosynthesis is initiated by condensation of a non-acetate propionyl-CoA starter unit and nine malonyl-CoA extender units to produce an unreduced decaketide (Fig. 4c), similarly to the metabolic pathway of the anticancer agent doxorubicin (Bao et al., 1999) (**4**). A conserved set of cyclases fold the polyketide in a manner similar to oxytetracycline (**5**) biosynthesis (Pickens and Tang, 2010). Deviations from the oxytetracycline paradigm are due to three additional genes that encode FAD-dependent proteins (Supplementary Table 1). These redox enzymes are likely to be responsible for the multiple skeletal rearrangements required for biosynthesis of mutaxanthenes.

Improving yields of mutaxanthenes. The structures of **1** and **3** differ only in regards to 7-O-methylation and the combined average product titer of mutaxanthenes was calculated to be on average 11 mg l^{-1} in the three first round mutant strains. In order to improve production, we performed a second round of SCMS and acquired 40 pure culture mutants to estimate the robustness of the methodology. Twenty mutants were selected by ranking them based on culture fluorescence and the metabolic profiles of these strains were estimated by HPLC-UV/Vis. The second round strains displayed significantly increased yields with an average production of 55 mg l^{-1} (Fig. 4d). The best performing mutant *A. orientalis* UV2(38) demonstrated 9.0-fold increased yields of 99 mg l^{-1} in comparison to the parental first round mutant *A. orientalis*

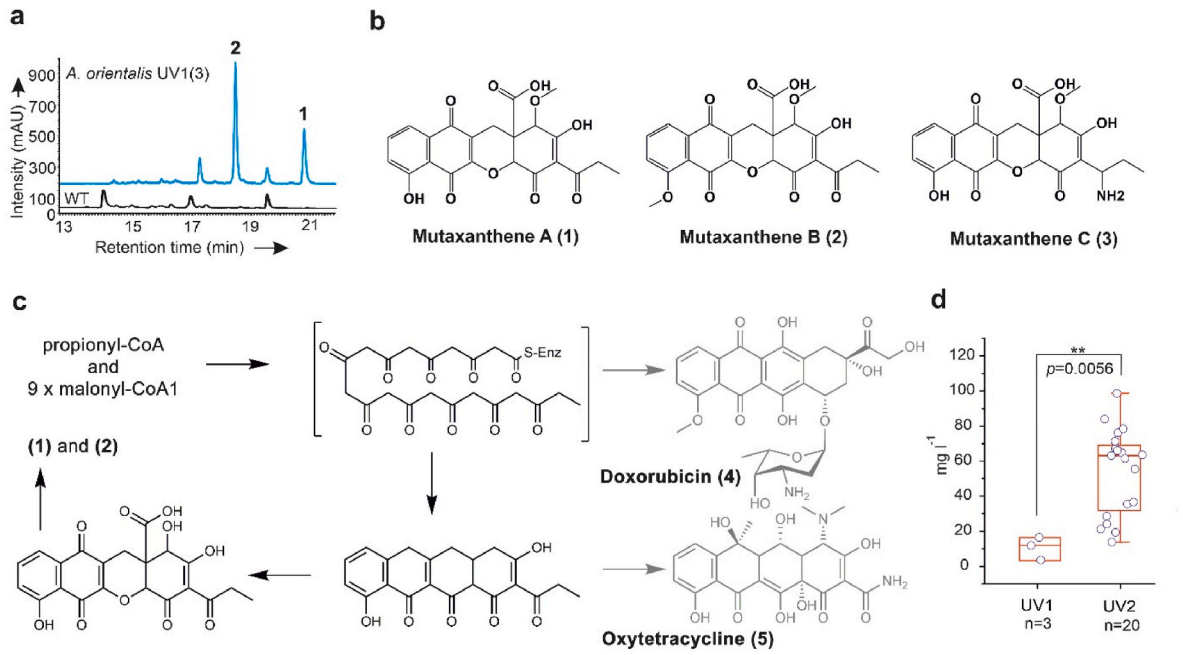

Fig. 4. Structure elucidation, biosynthesis and yield improvement of mutaxanthenes. a, Analysis of culture extracts by HPLC-UV/Vis indicates the production of two additional metabolites **1** and **2** in *A. orientalis* UV1(3) in comparison to the wild type. The chromatogram traces were recorded at 256 nm **b**, Chemical structures of mutaxanthenes A (**1**), B (**2**) and D (**3**) obtained from in *A. orientalis* UV1(3). **c**, The polyketide scaffolds of **1** and **2** are derived from propionyl-CoA started unit and nine malonyl-CoA extender units as in the biosynthesis of **4**. The set of cyclases encoded in the BBC that determine polyketide folding are related to the biosynthesis of **5**. A unique set of redox tailoring enzymes are utilized for multiple skeletal rearrangements that results in formation of **1** and **2**. **d**, Analysis of production profiles of 20 second round GFP-positive mutants demonstrate increased yields of **1** and **2**. Peak areas for the two metabolites obtained by HPLC were combined to reflect the total carbon flux to the activated pathway.

UV1(3).

3. Discussion

Biomanufacturing provides an important means for production of biomolecules for use in medicine and numerous industrial applications. The field is likely to significantly grow in the future due to advances in synthetic biology and a shift to green chemistry (Sadler, 2020). The commercial feasibility and success of these processes depend on product yields obtained from bioreactors. SCMS presents a generally applicable technology platform for industrial strain development of actinomycetes for production of pharmaceutical agents and industrial enzymes, where the efficiency of traditional strain development is increased by several orders of magnitude. Genome-wide mutagenesis is a proven method for increasing product yields (Miethke et al., 2021), but numerous cumulative mutations with significant variation between production strains (Peano et al., 2012, 2014) are typically required for generation of an overproducing phenotype. SCMS can probe large mutant libraries directly from liquid production medium to identify best candidate strains. The use of antibiotic selection in the removal of unwanted non- and low producing strains appears to be highly efficient, as demonstrated by the existence of very few individual mutant cells that are sfGFP negative in our mutagenesis libraries (Fig. 3b). Screening by FACS allows detection of the most promising strains from tens of millions of mutants. The combination of these two steps can be used to rapidly focus strain development efforts on the most promising fraction of the mutant library.

Actinomycetes are widely used for production of industrial enzymes due to good yields and protein solubility issues encountered in heterologous hosts (Sevillano et al., 2016). Even protein over-expression in model *Streptomyces* hosts from multi-copy number vectors and strong promoters does not guarantee good yields. As an example, over-expression of *choD* in *S. albus* J1074 using the integrative pSET152 vector and strong synthetic SP44 promoter led to approximately 3 – fold lower production of the cholesterol oxidase ChoD compared to *S. lavendulae* YAKB-15 wild type (Yamada et al., 2019). Expression studies in *S. lividans* TK 24 using the multicopy pIJ486 vector and *ermEp* promoter resulted in negligible production of ChoD with over 90-fold decrease in yield. Here we show that SCMS can be used to efficiently increase product titer of ChoD in the native host. The 5.0-fold yield enhancement is noteworthy, since *S. lavendulae* YAKB-15 has been reported to have the highest activity of a cell-associated cholesterol oxidase (Yamada et al., 2019). The combination of selection and ultra-high throughput screening may be sufficiently high for SCMS to replace medium optimization; we generated high-yield production strains in just three rounds of SCMS under preset culture conditions. The 22.8-fold yield enhancements obtained in GYM medium demonstrates the high dynamic range of the sfGFP reporter system. The strategy could be used to circumvent the need for exotic and hard to source medium ingredients required by industrial fermentation processes. One strain development cycle can be conducted in three-four weeks and iterative SCMS may provide a more cost effective approach for increasing production levels than conducting medium optimization experiments.

The discovery of numerous cryptic BGCs in actinomycetes has reinvigorated microbial natural product drug discovery pipelines (Panter et al., 2021). Computational genome mining is efficient in detection of potentially novel pathways (Medema and Fischbach, 2015), but robust methodologies for targeted activation of metabolic pathways have remained lacking. Cluster specific methodologies such as refactoring (Bauman et al., 2019), promoter exchange experiments (Zhang et al., 2017) and manipulation of regulatory elements (Ji et al., 2018) require extensive investments and are not easily scaled to handle multiple samples. Ideally, the technology should be able to probe entire genomes to induce changes at global regulatory levels, but also target specific BGCs identified by genome mining. Currently existing methodologies include variations of small molecule elicitors (Seyedsayamdost, 2014; Zhang and Seyedsayamdost, 2020), biosensors (Rebets et al., 2018) and other reporter guided (Yoshimura et al., 2020) systems. The key benefit

of SCMS over previous technologies is the ability to analyze several orders of magnitude larger mutant libraries, which is required since activation of a metabolic pathway is likely to be a rare event resulting from a combination of numerous mutations. Importantly, the SCMS protocol (Fig. 1) allows high-throughput work with multiple BGCs in parallel. Activation of the silent mutaxanthene pathway and yield enhancement via iterative rounds of SCMS to a yield of 99 mg l^{-1} demonstrates that SCMS can facilitate identification of metabolites from culture extracts and provide sufficient material for structure elucidation and bioactivity assays. In conclusion, SCMS is a new tool that offers a wide range of metabolic engineering applications to accelerate drug discovery and industrial production of proteins and natural products.

4. Methods

Reagents. All reagents were purchased from Sigma-Aldrich unless otherwise stated. All organic reagents used for HPLC and HR-MS were high-performance liquid chromatography (HPLC) grade solvents.

Strains and culture conditions. All plasmids were propagated (Sambrook and Russell, 2001) in *Escherichia coli* Top10 cultured in Luria-Bertani (LB) medium with apramycin (50 μg ml^{-1}) or kanamycin (50 μg ml^{-1}) at 37 °C. *E. coli* ET12567/pUZ8002 was used for conjugation (Bierman et al., 1992) and grown in LB at 37 °C with appropriate antibiotics (25 μg ml^{-1} chloramphenicol, 50 μg ml^{-1} kanamycin, 50 μg ml^{-1} apramycin). To prepare spores, *Streptomyces lavendulae* YAKB-15 and *Amycolatopsis orientalis* NRRL F3213 were cultivated on mannitol-soya flour agar (Kieser et al., 2000) plates at 30 °C.

Construction of reporter plasmids. Codon-optimized oligonucleotide fragment of s*fgfp* with strong synthetic promoter (SP44) and ribosome binding site (SR41) (Bai et al., 2015) flanking *Xba*I/*Spe*I restriction sites (fragment I), kanamycin and hygromycin resistance genes with corresponding ribosome binding sites flanking *Spe*I/*Bam*HI restriction sites (fragment II) and two fragments consisting of two strong terminator and promoter region of *choD* or *mut* operon linked to *gfp* partial sequence (1–234 bp) flanked with *Xba*I/*Nde*I restriction sites (fragments III), were ordered as synthetic fragments (ThermoFisher Scientific). First pSET152 plasmid and fragment I were digested by *Xba*I/*Spe*I restriction enzymes and two purified fragments were assembled with T4 DNA ligase according to standard protocol (Sambrook and Russell, 2001). Then, fragment II was digested with *Spe*I/*Bam*HI and ligated to the plasmid backbone to create pS_GK construct (*gfp* + kanamycin resistance gene). Reporter plasmids were constructed by digestion of fragment III with *Xba*I/*Nde*I and ligation to similarly cut pS_GK. The constructs were transformed into *S. lavendulae* and *A. orientalis* via conjugations.

Mutagenesis and selection. Chemical mutagenesis was carried out as described in Jones et al. (2017) with slight modifications. Spores (*circa* 10^8) of *S. lavendulae* harboring reporter probe were added to 1.5 ml of KPO_4 (0.01 M, pH 7.0) and exposed to 200 μl ethyl methanesulfonate to achieve 99% killing rate while H_2O was added to the control. The samples were vortexed for 30 s and incubated on shakers (300 rpm) at 30 °C for 1 h, with inversions performed in 10-min intervals. Then, the samples were centrifuged at 4000 rpm for 10 min at room temperature and subsequently the pellet was resuspended in one ml of freshly made and filter-sterilized 5% (w/v) sodium thiosulphate solution and then washed twice with 1 ml of H_2O and subsequently the pellet was resuspended in 1 ml H_2O. From each tube, a 10^{-4} dilution of the homogenate was made and 100 μl was plated onto MS plates and incubated for 3 day at 30 °C to estimate the killing rate. The rest of the homogenate was added to a 250 ml Erlenmeyer flask containing 25 ml of the antibiotic-free Y or GYM media and incubated on shaker at 300 rpm for 24 h at 30 °C. The mutant library and control strains were sub-cultured (500 μl inoculation) in 25 ml fresh media supplemented with varying concentrations of kanamycin 50–900 μg ml^{-1} in three-day intervals.

Quantitative Measurement of GFP Expression by Flow Cytometry. Mutant libraries of *S. lavendulae* and *A. orientalis* were subjected to FACS analysis to screen mutated single cells with the highest expression of GFP. Wild type strains and strains harboring strong s*fgfp* were used for FACS gating. Briefly, *Streptomyces* mycelia (3 day-old culture in 25 ml liquid media) were harvested (4 °C, 10,000×*g*, 5 min) and then the pellet were washed with MQ water three times and subsequently was suspended in 25 ml PBS buffer. The pellet was then subjected to ultrasonication (Bandelin Sonopuls HD 3100 homogeniser, microtip MS 73, diameter 13 mm, amplitude 20, pulse 10 s: stop 10 s, 5 min, on ice) to generate mycelia fragments. Fragments were then filtered through 5 ml Falcon® Polystyrene round bottom tubes with cell-strainer cap (Corning Science, Reynosa TAMP, Mexico). The fragmented mutated mycelia were analyzed by FACSAria Flow Cytometer with a 488-nm excitation laser and the FL1 (530/30 nm band-pass filter) detector. Each sample collected 50,000 events, and the data were acquired using BD FACSDiva™ 8.0.2 Software (BD Biosciences, CA) and analyzed by FlowJo™ v10.8 Software (BD Life Sciences). The parameters of the FACS setting were as follows: FSC-E00, SSC-650, FL1-400, FL2-400, threshold: FSC-50, SSC-400. The fluorescence of each sample was the geometric mean of all the measured cells and was normalized to the corresponding FSC value, which indicates the size of the cells. Single cells were sorted in 96 well plate containing GYM media, plated on MS-agar plates and streak plated to obtain pure cultures.

Cholesterol oxidase enzymatic assay. ChoD activity was measured spectrophotometrically as described previously (Yamada et al., 2019). The stoichiometric formation of H_2O_2 during the oxidation reaction of cholesterol was monitored with ABTS at 405 nm. To determine the cell-bound ChoD, 500 μl of cultures were centrifuged at 15,000×*g* for 10 min. The cell pellet was resuspended in extraction buffer (0.15% Tween 80 in 50 mM phosphate buffer solution) and mixed for 30 min at 4 °C. The suspension was centrifuged at 15,000×*g* and ChoD activity was measured from the supernatant. The activity assay mixture contained 120 μl Triton X-100 (0.05%) in 50 mM sodium-potassium phosphate buffer (pH 7), 10 μl ABTS (9.1 mM in MQ H_2O), 2.5 μl cholesterol in ethanol (1 mg ml^{-1}), 1.5 μl horseradish peroxidase solution (150 U ml^{-1}) and 20 μl of the extract preparation in a total volume of 154 μl. The spectrophotometric cholesterol activity assay was carried out in a 96-well plate. One unit of enzyme was defined as the amount of enzyme that forms 1 μmol of H_2O_2 per minute at pH 7.0 and 27 °C. All the samples including sorted cells, their corresponding control cultures and wild type strain were cultured in triplicates for 24 h in corresponding media and then subcultured into fresh media for 72 h (30 °C, 300 rpm).

Production and purification of mutaxanthenes. To produce **1**–**3**, 50 μl of mutant spores' stock (*A. orientalis*/pSGKP45_UV1(3)) were inoculated into 250 ml of TSB medium (2 flasks each with 250 ml) and grown for three days in a shaking incubator (30 °C, 300 rpm). The fully grown pre-culture was pooled together and 400 ml was transferred to 4 l of MS-broth and cultivated for 8 days (similar growth conditions) before being harvested. LXA1180 resin was added to the cultures to bind produced secondary metabolites. After cultivation, compounds were extracted from LXA1180 by first using 50% MeOH and then 90% MeOH. Both extracts were separately subjected to a liquid-liquid extraction by using $CHCl_3$ first without adjusting the pH. The neutral $CHCl_3$ was collected separately and the aqueous phase was further extracted twice with $CHCl_3$ after adding 1% (v/v) acetic acid. The $CHCl_3$ phases were dried and saved in −20 °C. The acidic $CHCl_3$ was subjected to a silica column (diameter 5.6 cm and length 9 cm) equilibrated with following conditions: toluene:ethyl acetate:methanol:formic acid 50:50:15:3. The first colorful front was collected in 90 ml fractions and 10 ml of ammonium actetate (1M) was added. The first four fractions were extracted using 1M ammonium acetate, the compounds of interest were in the aqueous phase. Next the aqueous phase was acidified using formic acid and acetic acid and extracted with $CHCl_3$. The $CHCl_3$ phases were dried, dissolved in methanol and injected to preparative HPLC, LC-20 AP with a diode array detector SPD-M20A (Shimadzu) with a reverse-phase column (Phenomenex, Kinetex) using a gradient from 15% acetonitrile with 0.1% formic acid to 100% acetonitrile. The peaks of interest were

collected, extracted with $CHCl_3$ and dried under vacuum and with nitrogen gas. NMR samples were prepared from overnight desiccated samples in $CDCl_3$ (**1**, **2**) or MeOD-*d4* (**3**).

Analyses of compounds by HPLC, NMR and HR-MS. HPLC analyses were carried out with a SCL-10Avp HPLC with an SPD-M10Avp diode array detector (Shimadzu) using a reversed-phase column (Phenomenex, Kinetex, 2.6 μm, 4.6 × 100 mm) using a gradient from 15% acetonitrile with 0.1% formic acid to 100% acetonitrile. NMR analysis was performed with a 600 MHz Bruker AVANCE-III NMR-system equipped with a liquid nitrogen cooled Prodigy TCI (inverted CryoProbe) at 298 K. The experiments included 1D (^1H, ^{13}C) and 2D measurements (COSY, HMBC, HSQCED, NOESY, TOCSY and 1,1-ADEQUATE). Topspin (Bruker Biospin) was used for spectral analysis and accurate chemical shifts and coupling constants were extracted with ChemAdder (Spin Discoveries Ltd.). High resolution mass (MicroTOF-Q, Bruker Daltonics) was performed with direct injection of purified compounds.

Transcriptional analysis by RT-PCR. To assess gene expression, *A. orientalis* NRRL F3213 wild type and an activated mutant (*A. orientalis*/pSGKP45_UV1(3)) were cultivated in 50 ml MS-liquid medium for 8 days. Sampling for RNA isolation was performed daily from 3d until 8d cultures. For this, 4 ml of the culture was harvested and gene expression was halted by addition of 444 μl stop solution (95% ethanol, 5% phenol). The mixture was incubated at room temperature for 15 min, followed by centrifugation (12,000×*g*, 15 min). The pellets were flash frozen in liquid nitrogen for storage at −80 °C until RNA was extracted.

Total RNA was extracted using the RNeasy Mini Kit (Qiagen) according to the manufacturer's instructions with minimal adjustments. Briefly, liquid nitrogen was employed to ground the cells to a powder. To the powder, 2 ml of phenol/$CHCl_3$/isoamyl alcohol (25:24:1) was added, followed by the addition of 1 ml TE (30 mM Tris-Cl, 1 mM EDTA, pH 8), and centrifuged (12,000×*g*, 6 min). The aqueous layer was extracted for a second time with 700 μl $CHCl_3$ and centrifuged (12,000×*g*, 4 min). To the upper layer (*circa.* 500 μl), 400 μl RLT and 500 μl of ethanol were added successively. The mixture was loaded onto the column, rinsed with 350 μl RW1, and then 80 μl of DNase I digest was applied to the column, followed by incubation at room temperature for 30 min before being washed with RW1 (350 μl) and RPE (500 μl, 2 times). Eventually, the column was eluted with 80 μl RNase-free water. The extracted mRNA was checked for purity on a 0.8% agarose gel and stored at −80 °C until further use.

Synthesis of cDNA from the extracted mRNA was performed using the ThermoScientific RevertAid First Strand cDNA synthesis kit with modest adjustments. Briefly, the 12 μl reaction contained 4 μg of template RNA, 1 μl of random hexamer primer, and DEPC water. This reaction mixture was incubated at 65 °C for 5 min, before being cooled on ice. To this mixture, 5 × reaction buffer (4 μl), RiboLock RNase inhibitor (20 U μl^{-1}, 1 μl), 10 mM dNTP mix (2 μl) and reverse transcriptase (200 U μl^{-1}, 1 μl) was added. The reaction mixture was incubated at 25 °C for 5 min, then at 42 °C for 65 min before being terminated by heating at 70 °C for 5 min.

RT-PCR amplification of the expressed gene targeting to the minimal polyketide synthase II gene regions was performed using the complementary DNA (cDNA) as a template and a pair of degenerate primers (5′-TSGCSTGCTTGGAYGCSATC-3′) (sense primer) and (5′-TGGAANCCGCCGAABCCGCT-3′) to amplify a product with the size of 613 bp (Metsä-Ketelä et al., 2002). PCR product was analyzed by gel electrophoresis on a 0.8% agarose gel stained with SybrSafe and compared to a one kb Plus Ladder (Invitrogen). RT-PCR amplifications was performed for all the samplings harvested, viz., from 3d until 8d for both wild type and the mutants. The 50 μl of the reaction mixture for the RT-PCR amplification contained cDNA (1000 × diluted): 1 μl, 10 × GC buffer: 10 μl, 10 mM dNTP mix: 2.5 μl, DMSO: 2.5 μl, Primers (2.5 μl each for forward and reverse), Dream Taq DNA polymerase: 0.5 μl, and DEPC water: 28.5 μl. The thermocycling conditions comprise an initial longer denaturation phase (96 °C, 2 min). The cycle steps for 30 cycles were as follows: denaturation (96 °C, 1 min), annealing (58 °C, 2 min), and extension (73 °C, 1.5 min). The reaction was terminated with a longer final extension (73 °C, 8.5 min). RT-PCR was performed on a SureCyler 8800 (Agilent Technologies, Santa Clara, California, USA). Conditions for the control reactions are described in the Supporting Information Text.

Accession numbers. The nucleotide sequences encoding the mutaxanthene were acquired from NCBI with the accession number JOIQ01000020.1. Nucleotide site for the '*mut*' gene cluster was identified to be between 183,729 and 216,609. The biosynthetic gene cluster encoding mutaxanthene from *A. orientalis* NRRL F3213 was deposited in MIBiG (Medema et al., 2015) under the accession number BGC0002137. Plasmid sequences for pSGK_P45_F3213 and pSGK_ChoD have been deposited to GenBank under the accession numbers ON497034 and ON497035, respectively.

Statistical analyses. All error bars shown in the present work are standard deviation values of three biological replicates. The number of replicates is provided in the corresponding figure caption. One-way analysis of variance (ANOVA) was used to demonstrate differences in values.

Author statement

Amir Akhgari and Bikash Baral conducted experiments, analyzed data and wrote the manuscript. Arina Koroleva, Vilja Siitonen, Charles Melançon III, David Fewer and Jani Rahkila conducted experiments and analyzed data. Mikko Metsä-Ketelä designed and conducted experiments, analyzed data, supervised the research and wrote the manuscript. All authors edited the manuscript.

Author contributions

A.A. and B.B. conducted experiments, analyzed data and wrote the manuscript. A.K., V.S., C.M., D.P.F. and J.R. conducted experiments and analyzed data. M.M.-K. designed and conducted experiments, analyzed data, supervised the research and wrote the manuscript. All authors edited the manuscript.

Declaration of competing interest

The authors declare no competing financial interests.

Acknowledgements

The financial support from the Jane and Aatos Erkko foundation to M.M.-K., Novo Nordisk Foundation (Grant number NNF21OC0068849) to M.M.-K. the Finnish Cultural Foundation to A.A. and the Turku University Foundation to B.B. is acknowledged. The authors would like to thank Wubin Gao, Džesika Pozlevičiūtė and Sazia Rahman for assistance in experimental analyses. We thank Tiina Pessa-Morikawa for assistance in flow sorting performed at the HiLife Flow Cytometry Viikki Sorting Unit, University of Helsinki.

Appendix A. Supplementary data

Supplementary data to this article can be found online at https://doi.org/10.1016/j.ymben.2022.07.002.

References

Adrio, J.L., Demain, A.L., 2006. Genetic improvement of processes yielding microbial products. FEMS Microbiol. Rev. 30, 187–214. https://doi.org/10.1111/j.1574-6976.2005.00009.x.

Albarano, L., Esposito, R., Ruocco, N., Costantini, M., 2020. Genome mining as new challenge in natural products discovery. Mar. Drugs 18, 199. https://doi.org/10.3390/md18040199.

Årdal, C., Balasegaram, M., Laxminarayan, R., McAdams, D., Outterson, K., Rex, J.H., Sumpradit, N., 2019. Antibiotic development — economic, regulatory and societal challenges. Nat. Rev. Microbiol. 18, 267–274. https://doi.org/10.1038/s41579-019-0293-3.

Askenazi, M., Driggers, E.M., Holtzman, D.A., Norman, T.C., Iverson, S., Zimmer, D.P., Boers, M.-E.E., Blomquist, P.R., Martinez, E.J., Monreal, A.W., Feibelman, T.P., Mayorga, M.E., Maxon, M.E., Sykes, K., Tobin, J.V., Cordero, E., Salama, S.R., Trueheart, J., Royer, J.C., Madden, K.T., 2003. Integrating transcriptional and metabolite profiles to direct the engineering of lovastatin-producing fungal strains. Nat. Biotechnol. 21, 150–156. https://doi.org/10.1038/nbt781.

Bai, C., Zhang, Y., Zhao, X., Hu, Y., Xiang, S., Miao, J., Lou, C., Zhang, L., Demain, A.L., 2015. Exploiting a precise design of universal synthetic modular regulatory elements to unlock the microbial natural products in *Streptomyces*. Proc. Natl. Acad. Sci. U.S.A. 112, 12181–12186. https://doi.org/10.1073/pnas.1511027112.

Baltz, R.H., 1978. Genetic recombination in *Streptomyces fradiae* by protoplast fusion and cell regeneration. J. Gen. Microbiol. 107, 93–102. https://doi.org/10.1099/00221287-107-1-93.

Bandyopadhyay, A.A., Khetan, A., Malmberg, L.H., Zhou, W., Hu, W.S., 2017. Advancement in bioprocess technology: parallels between microbial natural products and cell culture biologics. J. Ind. Microbiol. Biotechnol. 44, 785–797. https://doi.org/10.1007/s10295-017-1913-4.

Bao, W., Sheldon, P.J., Hutchinson, C.R., 1999. Purification and properties of the *Streptomyces peucetius* DpsC β- ketoacyl:acyl carrier protein synthase III that specifies the propionate- starter unit for type II polyketide biosynthesis. Biochemistry 38, 9752–9757. https://doi.org/10.1021/bi990751h.

Baral, B., Akhgari, A., Metsä-Ketelä, M., 2018. Activation of microbial secondary metabolic pathways: avenues and challenges. Synth. Syst. Biotechnol. 3, 163–178. https://doi.org/10.1016/j.synbio.2018.09.001.

Bauman, K.D., Li, J., Murata, K., Mantovani, S.M., Dahesh, S., Nizet, V., Luhavaya, H., Moore, B.S., 2019. Refactoring the cryptic streptophenazine biosynthetic gene cluster unites phenazine, polyketide, and nonribosomal peptide biochemistry. Cell Chem. Biol. 26, 724–736. https://doi.org/10.1016/j.chembiol.2019.02.004 e7.

Bierman, M., Logan, R., O'Brien, K., Seno, E.T., Nagaraja Rao, R., Schoner, B.E., 1992. Plasmid cloning vectors for the conjugal transfer of DNA from *Escherichia coli* to *Streptomyces* spp. Gene 116, 43–49. https://doi.org/10.1016/0378-1119(92)90627-2.

Binder, S., Schendzielorz, G., Stäbler, N., Krumbach, K., Hoffmann, K., Bott, M., Eggeling, L., 2012. A high-throughput approach to identify genomic variants of bacterial metabolite producers at the single-cell level. Genome Biol. 13, R40. https://doi.org/10.1186/gb-2012-13-5-r40.

Cao, X., Luo, Z., Zeng, W., Xu, S., Zhao, L., Zhou, J., 2018. Enhanced avermectin production by *Streptomyces avermitilis* ATCC 31267 using high-throughput screening aided by fluorescence-activated cell sorting. Appl. Microbiol. Biotechnol. 102, 703–712. https://doi.org/10.1007/s00253-017-8658-x.

Chen, Y.-J., Liu, P., Nielsen, A.A.K., Brophy, J.A.N., Clancy, K., Peterson, T., Voigt, C.A., 2013. Characterization of 582 natural and synthetic terminators and quantification of their design constraints. Nat. Methods 10, 659–664. https://doi.org/10.1038/nmeth.2515.

Derewacz, D.K., Goodwin, C.R., McNees, C.R., McLean, J.A., Bachmann, B.O., 2013. Antimicrobial drug resistance affects broad changes in metabolomic phenotype in addition to secondary metabolism. Proc. Natl. Acad. Sci. U.S.A. 110, 2336–2341. https://doi.org/10.1073/pnas.1218524110.

Genilloud, O., 2017. Actinomycetes: still a source of novel antibiotics. Nat. Prod. Rep. 34, 1203–1232. https://doi.org/10.1039/c7np00026j.

Guo, F., Xiang, S., Li, L., Wang, B., Rajasärkkä, J., Gröndahl-Yli-Hannuksela, K., Ai, G., Metsä-Ketelä, M., Yang, K., 2015. Targeted activation of silent natural product biosynthesis pathways by reporter-guided mutant selection. Metab. Eng. 28, 134–142. https://doi.org/10.1016/j.ymben.2014.12.006.

Horbal, L., Siegl, T., Luzhetskyy, A., 2018. A set of synthetic versatile genetic control elements for the efficient expression of genes in Actinobacteria. Sci. Rep. 8, 491. https://doi.org/10.1038/s41598-017-18846-1.

Ji, C.-H., Kim, J.-P., Kang, H.-S., 2018. Library of synthetic *Streptomyces* regulatory sequences for use in promoter engineering of natural product biosynthetic gene clusters. ACS Synth. Biol. 7, 1946–1955. https://doi.org/10.1021/acssynbio.8b00175.

Jones, S.E., Ho, L., Rees, C.A., Hill, J.E., Nodwell, J.R., Elliot, M.A., 2017. *Streptomyces* exploration is triggered by fungal interactions and volatile signals. Elife 6, 1–21. https://doi.org/10.7554/eLife.21738.

Kieser, T., Bibb, M.J., Buttner, M.J., Chater, K.F., Da, H., Kieser, T., Bibb, M., Buttner, M., Chater, K., Bibb, M.J., Buttner, M.J., Chater, K.F., Da, H., 2000. Practical *Streptomyces* Genetics, second ed. John Innes Centre. John Innes Centre, UK.

Li, P., Guo, Z., Tang, W., Chen, Y., 2018. Activation of three natural product biosynthetic gene clusters from *Streptomyces lavendulae* CGMCC 4.1386 by a reporter-guided strategy. Synth. Syst. Biotechnol. 3, 254–260. https://doi.org/10.1016/j.synbio.2018.10.010.

Mann, J., 2001. Natural products as immunosuppressive agents. Nat. Prod. Rep. 18, 417–430. https://doi.org/10.1039/b001720p.

Manteca, A., Alvarez, R., Salazar, N., Yagüe, P., Sanchez, J., 2008. Mycelium differentiation and antibiotic production in submerged cultures of *Streptomyces coelicolor*. Appl. Environ. Microbiol. 74, 3877–3886. https://doi.org/10.1128/AEM.02715-07.

Medema, M.H., de Rond, T., Moore, B.S., 2021. Mining genomes to illuminate the specialized chemistry of life. Nat. Rev. Genet. 22, 553–571. https://doi.org/10.1038/s41576-021-00363-7.

Medema, M.H., Fischbach, M.A., 2015. Computational approaches to natural product discovery. Nat. Chem. Biol. 11, 639–648. https://doi.org/10.1038/nchembio.1884.

Medema, M.H., Kottmann, R., Yilmaz, P., Cummings, M., Biggins, J.B., Blin, K., De Bruijn, I., Chooi, Y.H., Claesen, J., Coates, R.C., Cruz-Morales, P., Duddela, S., Düsterhus, S., Edwards, D.J., Fewer, D.P., Garg, N., Geiger, C., Gomez-Escribano, J. P., Greule, A., Hadjithomas, M., Haines, A.S., Helfrich, E.J.N., Hillwig, M.L., Ishida, K., Jones, A.C., Jones, C.S., Jungmann, K., Kegler, C., Kim, H.U., Kötter, P., Krug, D., Masschelein, J., Melnik, A.V., Mantovani, S.M., Monroe, E.A., Moore, M., Moss, N., Nützmann, H.W., Pan, G., Pati, A., Petras, D., Reen, F.J., Rosconi, F., Rui, Z., Tian, Z., Tobias, N.J., Tsunematsu, Y., Wiemann, P., Wyckoff, E., Yan, X., Yim, G., Yu, F., Xie, Y., Aigle, B., Apel, A.K., Balibar, C.J., Balskus, E.P., Barona-Gómez, F., Bechthold, A., Bode, H.B., Borriss, R., Brady, S.F., Brakhage, A.A., Caffrey, P., Cheng, Y.Q., Clardy, J., Cox, R.J., De Mot, R., Donadio, S., Donia, M.S., Van Der Donk, W.A., Dorrestein, P.C., Doyle, S., Driessen, A.J.M., Ehling-Schulz, M., Entian, K.D., Fischbach, M.A., Gerwick, L., Gerwick, W.H., Gross, H., Gust, B., Hertweck, C., Höfte, M., Jensen, S.E., Ju, J., Katz, L., Kaysser, L., Klassen, J.L., Keller, N.P., Kormanec, J., Kuipers, O.P., Kuzuyama, T., Kyrpides, N.C., Kwon, H.J., Lautru, S., Lavigne, R., Lee, C.Y., Linquan, B., Liu, X., Liu, W., Luzhetskyy, A., Mahmud, T., Mast, Y., Méndez, C., Metsä-Ketelä, M., Micklefield, J., Mitchell, D.A., Moore, B.S., Moreira, L.M., Müller, R., Neilan, B.A., Nett, M., Nielsen, J., O'Gara, F., Oikawa, H., Osbourn, A., Osburne, M.S., Ostash, B., Payne, S.M., Pernodet, J.L., Petricek, M., Piel, J., Ploux, O., Raaijmakers, J.M., Salas, J.A., Schmitt, E.K., Scott, B., Seipke, R.F., Shen, B., Sherman, D.H., Sivonen, K., Smanski, M.J., Sosio, M., Stegmann, E., Süssmuth, R.D., Tahlan, K., Thomas, C.M., Tang, Y., Truman, A.W., Viaud, M., Walton, J.D., Walsh, C.T., Weber, T., Van Wezel, G.P., Wilkinson, B., Willey, J.M., Wohlleben, W., Wright, G.D., Ziemert, N., Zhang, C., Zotchev, S.B., Breitling, R., Takano, E., Glöckner, F.O., 2015. Minimum information about a biosynthetic gene cluster. Nat. Chem. Biol. 11, 625–631. https://doi.org/10.1038/nchembio.1890.

Metsä-Ketelä, M., Halo, L., Munukka, E., Hakala, J., Mäntsäla, P., Ylihonko, K., 2002. Molecular evolution of aromatic polyketides and comparative sequence analysis of polyketide ketosynthase and 16S ribosomal DNA genes from various *Streptomyces* species. Appl. Environ. Microbiol. 68, 4472–4479. https://doi.org/10.1128/AEM.68.9.4472-4479.2002.

Miethke, M., Pieroni, M., Weber, T., Brönstrup, M., Hammann, P., Halby, L., Arimondo, P.B., Glaser, P., Aigle, B., Bode, H.B., Moreira, R., Li, Y., Luzhetskyy, A., Medema, M.H., Pernodet, J.L., Stadler, M., Tormo, J.R., Genilloud, O., Truman, A. W., Weissman, K.J., Takano, E., Sabatini, S., Stegmann, E., Brötz-Oesterhelt, H., Wohlleben, W., Seemann, M., Empting, M., Hirsch, A.K.H., Loretz, B., Lehr, C.M., Titz, A., Herrmann, J., Jaeger, T., Alt, S., Hesterkamp, T., Winterhalter, M., Schiefer, A., Pfarr, K., Hoerauf, A., Graz, H., Graz, M., Lindvall, M., Ramurthy, S., Karlén, A., van Dongen, M., Petkovic, H., Keller, A., Peyrane, F., Donadio, S., Fraisse, L., Piddock, L.J.V., Gilbert, I.H., Moser, H.E., Müller, R., 2021. Towards the sustainable discovery and development of new antibiotics. Nat. Rev. Chem 5, 726–749. https://doi.org/10.1038/s41570-021-00313-1.

Minas, W., 2005. Production of erythromycin with Saccharopolyspora erythraea. In: Microbial Processes and Products. Humana Press, Totowa, NJ, pp. 65–90. https://doi.org/10.1385/1-59259-847-1:065.

Mukhtar, S., Zaheer, A., Aiysha, D., Abdulla Malik, K., Mehnaz, S., 2017. Actinomycetes: a source of industrially important enzymes. J. Proteonomics Bioinf. 10, 316–319. https://doi.org/10.4172/jpb.1000456.

Nakano, M.M., Mashiko, H., Ogawara, H., 1984. Cloning of the kanamycin resistance gene from a kanamycin-producing *Streptomyces* species. J. Bacteriol. 157, 79–83. https://doi.org/10.1128/jb.157.1.79-83.1984.

Newman, D.J., Cragg, G.M., 2020. Natural products as sources of new drugs over the nearly four decades from 01/1981 to 09/2019. J. Nat. Prod. 83, 770–803. https://doi.org/10.1021/acs.jnatprod.9b01285.

Ogasawara, Y., Yackley, B.J., Greenberg, J.A., Rogelj, S., Melançon, C.E., 2015. Expanding our understanding of sequence-function relationships of Type II polyketide biosynthetic gene clusters: bioinformatics-guided identification of frankiamicin a from *Frankia* sp. EAN1pec. PLoS One 10, 1–25. https://doi.org/10.1371/journal.pone.0121505.

Panter, F., Bader, C.D., Müller, R., 2021. Synergizing the potential of bacterial genomics and metabolomics to find novel antibiotics. Chem. Sci. 12, 5994–6010. https://doi.org/10.1039/d0sc06919a.

Peano, C., Damiano, F., Forcato, M., Pietrelli, A., Palumbo, C., Corti, G., Siculella, L., Fuligni, F., Tagliazucchi, G.M., De Benedetto, G.E., Bicciato, S., De Bellis, G., Alifano, P., 2014. Comparative genomics revealed key molecular targets to rapidly convert a reference rifamycin-producing bacterial strain into an overproducer by genetic engineering. Metab. Eng. 26, 1–16. https://doi.org/10.1016/j.ymben.2014.08.001.

Peano, C., Talà, A., Corti, G., Pasanisi, D., Durante, M., Mita, G., Bicciato, S., De Bellis, G., Alifano, P., 2012. Comparative genomics and transcriptional profiles of *Saccharopolyspora erythraea* NRRL 2338 and a classically improved erythromycin over-producing strain. Microb. Cell Factories 11, 32. https://doi.org/10.1186/1475-2859-11-32.

Pickens, L.B., Tang, Y., 2010. Oxytetracycline biosynthesis. J. Biol. Chem. 285, 27509–27515. https://doi.org/10.1074/jbc.R110.130419.

Prakash, D., Nawani, N., Prakash, M., Bodas, M., Mandal, A., Khetmalas, M., Kapadnis, B., 2013. Actinomycetes: a repertory of green catalysts with a potential revenue resource. BioMed Res. Int. https://doi.org/10.1155/2013/264020, 2013.

Ramirez, M.S., Tolmasky, M.E., 2010. Aminoglycoside modifying enzymes. Drug Resist. Updates 13, 151–171. https://doi.org/10.1016/j.drup.2010.08.003.

Rebets, Y., Schmelz, S., Gromyko, O., Tistechok, S., Petzke, L., Scrima, A., Luzhetskyy, A., 2018. Design, development and application of whole-cell based antibiotic-specific biosensor. Metab. Eng. 47, 263–270. https://doi.org/10.1016/j.ymben.2018.03.019.

Sadler, J.C., 2020. The Bipartisan future of synthetic chemistry and synthetic biology. Chembiochem 21, 3489–3491. https://doi.org/10.1002/cbic.202000418.
Sambrook, J., Russell, D., 2001. Molecular Cloning: A Laboratory Manual, third ed. Cold Spring Harbor Laboratory Press, Cold Spring Harbor (NY).
Sekurova, O.N., Sun, Y.-Q., Zehl, M., Rückert, C., Stich, A., Busche, T., Kalinowski, J., Zotchev, S.B., 2021. Coupling of the engineered DNA "mutator" to a biosensor as a new paradigm for activation of silent biosynthetic gene clusters in *Streptomyces*. Nucleic Acids Res. 49, 8396–8405. https://doi.org/10.1093/nar/gkab583.
Sevillano, L., Vijgenboom, E., van Wezel, G.P., Díaz, M., Santamaría, R.I., 2016. New approaches to achieve high level enzyme production in *Streptomyces lividans*. Microb. Cell Factories 15, 28. https://doi.org/10.1186/s12934-016-0425-7.
Seyedsayamdost, M.R., 2014. High-throughput platform for the discovery of elicitors of silent bacterial gene clusters. Proc. Natl. Acad. Sci. U.S.A. 111, 7266–7271. https://doi.org/10.1073/pnas.1400019111.
Shiomi, K., Omura, S., 2004. Antiparasitic agents produced by microorganisms. Proc. Japan Acad. Ser. B 80, 245–258. https://doi.org/10.2183/pjab.80.245.
Stonesifer, J., Baltz, R.H., 1985. Mutagenic DNA repair in *Streptomyces*. Proc. Natl. Acad. Sci. U.S.A. 82, 1180–1183. https://doi.org/10.1073/pnas.82.4.1180.
Thirsk, C., Whiting, A., 2002. Polyene natural products. J. Chem. Soc. Perkin Trans. 1, 999–1023. https://doi.org/10.1039/b109741p.
van der Meij, A., Worsley, S.F., Hutchings, M.I., van Wezel, G.P., 2017. Chemical ecology of antibiotic production by actinomycetes. FEMS Microbiol. Rev. 41, 392–416. https://doi.org/10.1093/femsre/fux005.
van der Zanden, S.Y., Qiao, X., Neefjes, J., 2021. New insights into the activities and toxicities of the old anticancer drug doxorubicin. FEBS J. 288, 6095–6111. https://doi.org/10.1111/febs.15583.
van Veluw, G.J., Petrus, M.L.C., Gubbens, J., de Graaf, R., de Jong, I.P., van Wezel, G.P., Wösten, H.A.B., Claessen, D., 2012. Analysis of two distinct mycelial populations in liquid-grown *Streptomyces* cultures using a flow cytometry-based proteomics approach. Appl. Microbiol. Biotechnol. 96, 1301–1312. https://doi.org/10.1007/s00253-012-4490-5.
Van Wezel, G.P., McDowall, K.J., 2011. The regulation of the secondary metabolism of Streptomyces: new links and experimental advances. Nat. Prod. Rep. 28, 1311–1333. https://doi.org/10.1039/c1np00003a.
Wagner, J.M., Liu, L., Yuan, S.-F., Venkataraman, M.V., Abate, A.R., Alper, H.S., 2018. A comparative analysis of single cell and droplet-based FACS for improving production phenotypes: riboflavin overproduction in *Yarrowia lipolytica*. Metab. Eng. 47, 346–356. https://doi.org/10.1016/j.ymben.2018.04.015.
Wang, Y., Tao, Z., Zheng, H., Zhang, F., Long, Q., Deng, Z., Tao, M., 2016. Iteratively improving natamycin production in *Streptomyces gilvosporeus* by a large operon-reporter based strategy. Metab. Eng. 38, 418–426. https://doi.org/10.1016/j.ymben.2016.10.005.
Wendisch, V.F., 2014. Microbial production of amino acids and derived chemicals: synthetic biology approaches to strain development. Curr. Opin. Biotechnol. 30, 51–58. https://doi.org/10.1016/j.copbio.2014.05.004.
Wietzorrek, A., Bibb, M., 1997. A novel family of proteins that regulates antibiotic production in streptomycetes appears to contain an OmpR-like DNA-binding fold. Mol. Microbiol. 25, 1181–1184.
Xiang, S.-H.H., Li, J., Yin, H., Zheng, J.-T.T., Yang, X., Wang, H.-B. Bin, Luo, J.-L.L., Bai, H., Yang, K.-Q.Q., 2009. Application of a double-reporter-guided mutant selection method to improve clavulanic acid production in *Streptomyces clavuligerus*. Metab. Eng. 11, 310–318. https://doi.org/10.1016/j.ymben.2009.06.003.
Yamada, K., Koroleva, A., Laughlin, M., Oksanen, N., Akhgari, A., Safronova, V., Yakovleva, E., Kolodyaznaya, V., Buldakova, T., Metsä-Ketelä, M., 2019. Characterization and overproduction of cell-associated cholesterol oxidase ChoD from *Streptomyces lavendulae* YAKB-15. Sci. Rep. 9, 11850 https://doi.org/10.1038/s41598-019-48132-1.
Yoshimura, A., Covington, B.C., Gallant, É., Zhang, C., Li, A., Seyedsayamdost, M.R., 2020. Unlocking cryptic metabolites with mass spectrometry-guided transposon mutant selection. ACS Chem. Biol. 15, 2766–2774. https://doi.org/10.1021/acschembio.0c00558.
Zalacain, M., González, A., Guerrero, M.C., Mattaliano, R.J., Malpartida, F., Jiménez, A., 1986. Nucleotide sequence of tbe hygromycin B phosphotransferase gene from *Streptomyces hygroscopicus*. Nucleic Acids Res. 14, 1565–1581. https://doi.org/10.1093/nar/14.4.1565.
Zhang, C., Seyedsayamdost, M.R., 2020. Discovery of a cryptic depsipeptide from *Streptomyces ghanaensis* via MALDI-MS-guided high-throughput elicitor screening. Angew. Chem. Int. Ed. 59, 23005–23009. https://doi.org/10.1002/anie.202009611.
Zhang, M.M., Wong, F.T., Wang, Y., Luo, S., Lim, Y.H., Heng, E., Yeo, W.L., Cobb, R.E., Enghiad, B., Ang, E.L., Zhao, H., 2017. CRISPR-Cas9 strategy for activation of silent *Streptomyces* biosynthetic gene clusters. Nat. Chem. Biol. 13, 607–609. https://doi.org/10.1038/nchembio.2341.